ELSEVIER

Journal of Luminescence 94–95 (2001) 569–573

JOURNAL OF LUMINESCENCE

www.elsevier.com/locate/jlumin

Femtosecond pump–probe spectroscopy of the dendrimeric nanostar

Andreas Tortschanoff, Andrei Piryatinski, Shaul Mukamel*

Department of Chemistry, University of Rochester, Rochester, NY 14627, USA

Abstract

The nonlinear exciton equations combined with the doorway–window formalism were used to calculate the pump–probe signal in the extended nanostar. The results are compared to previous time resolved fluorescence calculations. In addition to the signatures of single-exciton energy funneling from the periphery towards the center, the pump–probe signal also carries useful information about two exciton states. © 2001 Published by Elsevier Science B.V.

Keywords: Dendrimer; Nanostar; Pump–probe; Spectroscopy; Energy funneling

Dendrimers are highly ordered branched macromolecules which have attracted much theoretical and experimental attention [1]. Apart from the fundamental interest in their unusual transport and optical properties, they are promising candidates for a wide variety of applications, including electro-optical organic light sources [2], drug delivery systems [3,4] and nanoscale optical sensors [5,6].

In this paper we study a phenylethynylperylene-terminated phenylacetylene dendrimer derivative, called the nanostar [6,7] (Fig. 1), where one of the three dendrimer branches is substitued by a perylene unit which can act as an exciton trap, collecting the photoexcited electron–hole pairs initially formed in the dendrimer lattice. The molecule has four generations of phenylacatylene units with decreasing lengths creating an efficient energy funnel towards the trap.

Recent experimental [6] and theoretical [8] investigations have shown that the excitons in this family of dendrimers are localized to the linear segments, since the meta-branching on the phenylene bridges inhibits effective delocalization. This allows to model this system using a Frenkel exciton Hamiltonian with coulombic coupling between excitations localized on the linear segments.

The signatures of energy funneling in the time and frequency-gated fluorescence signal in dendrimers were studied in a recent paper [9]. A Frenkel Hamiltonian with parameters based on CEO calculations [10] was computed and used to solve the equations of motions for a hierarchy of exciton oscillators (nonlinear exciton equations [11]). Exciton transport was described using Redfield theory [12,13], where the effects of nuclear motion are incorporated through relaxation superoperators, calculated perturbatively in the

*Corresponding author. Fax: +1-716-473-6889.
E-mail address: mukamel@chem.rochester.edu (S. Mukamel).

0022-2313/01/$ - see front matter © 2001 Published by Elsevier Science B.V.
PII: S0022-2313(01)00389-1

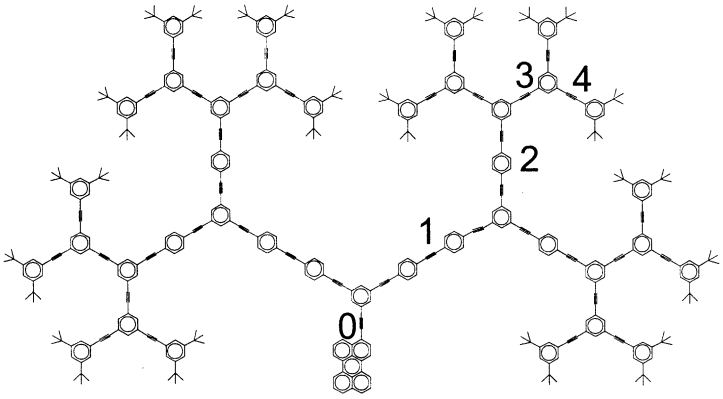

Fig. 1. The nanostar molecule. The numbers indicate the generations.

exciton–phonon coupling. The signal was calculated in the doorway–window representation of sequential four wave mixing spectroscopies [14,15].

In this paper we will compare the fluorescence signal with calculations of multi-color pump–probe experiments, where the system interacts twice with a pump pulse and the signal is produced by another interaction with a delayed probe pulse. Pump–probe spectra can be described using the doorway–window formalism [15,16] provided the pump and the probe pulse are temporally well separated. Such experiments yield additional information unavailable from time resolved fluorescence.

The doorway–window expression for the sequential pump–probe signal S_{pp} was derived in Refs. [15,16] and is given by

$$S_{\mathrm{pp}}(\tau,\omega_2,\omega_1)=\sum_{mnkl}\int_0^\infty \mathrm{d}\tau'\int_0^\infty \mathrm{d}t_2\ \mathscr{W}_{mn}\quad(\tau-\tau',\omega_2)G^{(N)}_{mn,\,kl}(t_2)\mathscr{D}_{kl}(\tau'-t_2,\omega_1). \qquad (1)$$

Here ω_1 (ω_2) are the pump (probe) carrier frequencies and τ is the pump/probe delay. m, n, k, $l=1,\ldots,31$ denote the various segments. $\mathscr{D}_{kl}$ is the *doorway wavepacket*, representing the exciton density matrix prepared by the pump. $\mathscr{W}_{mn}$ is the *window wavepacket* created from the ground, the one-, and the two-exciton states by two interactions with the probe. $G^{(N)}$ represents the propagation of the doorway wavepacket during τ. This representation provides an intuitive physical description that separates the process into preparation, propagation, and detection of the excitonic wavepacket. The doorway wavepacket is the reduced one-exciton density matrix containing the initially prepared exciton populations and coherences. The signal is given by the Liouville space overlap of this wavepacket, propagated for the delay period, with the window. The window also involves transitions from single- to two-exciton states and carries valuable information about two-exciton dynamics. Single color pump–probe experiments on nanostars were reported recently [17].

We have simulated the exciton dynamics and the pump–probe signal of the extended nanostar. The two–exciton states are not calculated explicitly but the pump–probe signal is directly obtained from the nonlinear exciton equations and expressed in terms of the scattering matrix [11]. The process is viewed as a scattering between quasiparticles, single excitons, which results from their non-boson behavior, rather than a transition between different states. The molecular parameters are taken from previous CEO calculations [10]. The overdamped Brownian oscillator model [15] for the bath was used to compute the Redfield matrix. All calculations were performed at room temperature $T=300\,\mathrm{K}$ with the same model parameters as used in Ref. [9].

The pump pulse with a Gaussian profile with variance $\sigma=20\,\mathrm{fs}$ is tuned to $\omega\sim 29{,}100\,\mathrm{cm}^{-1}$ to be on resonance with the highest periphery exciton.

The probe was assumed to be both monochromatic and very short (i.e. in the snapshot limit [16]) which allows to spectrally resolve the signal at variable time delays.

Fig. 2(a) shows the oscillator strengths of the single-exciton states. There are 31 states, however some of them are degenerate or have negligible dipole moments. The low energy trap as well as the high energy peripherial states are energetically well separated from the other generations. Even though most of the exciton lines in the nanostar are too close to be resolved, we find distinct bands in the calculated absorption spectrum (dotted line) that can be attributed to excitons localized on different generations [9].

In Fig. 3 we compare the time resolved fluorescence spectra [9] with the pump–probe signals for different delay times τ, as indicated. Initially the fluorescence signal only shows emission from the high energy excitons that were directly excited. The exciton wavepacket then gradually funnels to the trap via generations 2 and 1. After 50 ps most of the excitation has reached the trap and after 100 ps the fluorescence signal is nearly exclusively emitted by the trap. In a similar way the propagation of the doorway wavepacket is monitored in the pump–probe technique. The right column in Fig. 3 shows the spectrally resolved pump–probe signal following excitation of the peripheral segments. Negative signal corresponds to reduced absorption (i.e. increased transmission) due to hole burning (HB) and stimulated emission (SE). Positive signals result from excited state absorption (ESA). The energy funneling shows up in a very clear and intuitive way. Populated exciton states show negative HB and SE signals at the corresponding transition energies. The localization on the periphery within the first ps is indicated by the negative signal at $\sim 29{,}100\,\mathrm{cm}^{-1}$. The excitation then moves towards lower energy sites populating the second and first generation, finally reaching the perylene trap. After ~ 100 ps the only negative contribution comes from the perylene site, indicating complete funneling. From the negative bands in the pump–probe spectra we can directly observe and quantify the funneling process of the exciton populations towards lower energy states, and recover all the information obtained from fluorescence. However, the pump–probe signal also shows ESA where two-exciton states are involved. While HB and SE result exclusively from single–exciton states, and thus follow the exciton dynamics in the same way as time resolved fluorescence, the positive ESA bands are a new feature of pump–probe septra. In the exciton state picture, the ESA probes transitions from a one-exciton state to a two-exciton state. In the chromophore representation this means that the excitation of one chromophore changes the absorption behavior of a different chromophore due to their mutual interaction. Information about the two-exciton resonances originating from interactions between excitons are contained in the poles of the exciton scattering matrix [18].

To clearly highlight the various contributions to the transient absorption signal of Fig. 3(b) we repeated the simulations with a narrow line width $\Gamma = 8\,\mathrm{cm}^{-1}$, where the different bands are well resolved and can be assigned [19]. The resulting

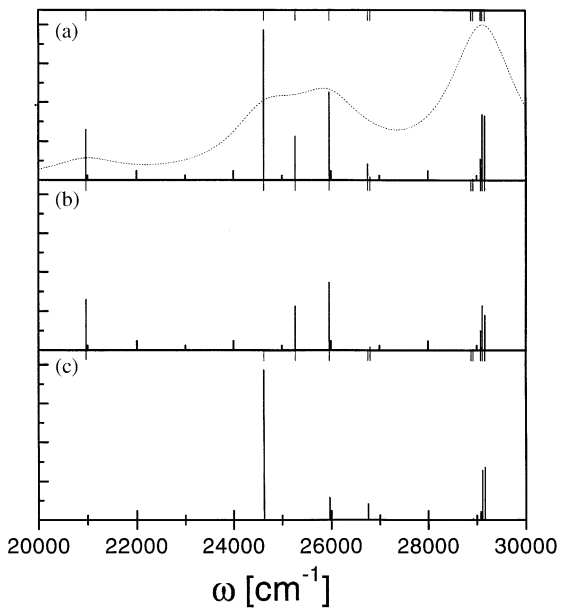

Fig. 2. The stick spectra show the individual one-exciton energies and oscillator strengths: (a) unpolarized (the dotted line shows the calculated absorption spectrum for a width $\Gamma \sim 800\,\mathrm{cm}^{-1}$), (b) parallel and (c) perpendicular to the trap's transition dipole moment.

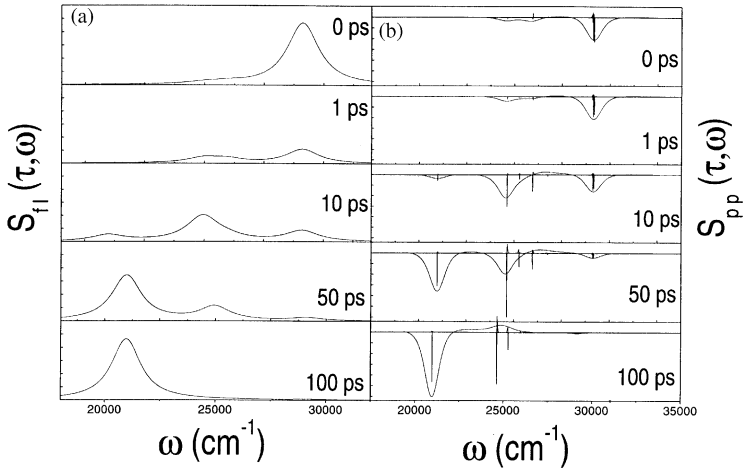

Fig. 3. (a) Dispersed fluorescence and (b) pump–probe signals from the nanostar at various delay times. See text for details.

signal also depicted in Fig. 3 shows the energy funneling and a complicated interplay of positive and negative contributions. The ESA contributions are energetically very close and overlap with the SE and HB contributions.

The absence of a positive signal close to the perylene line indicates that the trap is only weakly coupled to the other generations so that excitation of the rest of the dendrimer does not significantly influence the absorption of the perylene exciton. However, when the excitation is localized on the trap, we see its influences on excitons 1 and 2 at the two ESA bands at 24,667 and 25,225 cm^{-1}.

Further information can be obtained from polarized pulses and oriented samples. Fig. 4 shows the spectrally resolved pump–probe signal for different time delays for parallel and perpendicular polarizations of pump and probe pulse. We again tuned the pump to excite the periphery. Fig. 4(a) (left column) corresponds to the case where both pump and probe pulse are polarized parallel to the dipole of the perylene site and the right column presents the case where the pump is parallel and the probe is perpendicular. From Fig. 2 we expect very different states to be probed in both configurations. If e.g. a pulse is parallel to the transition dipole of the trap it will be perpendicular to the transition dipole of the first exciton, which carries most of the oscillator strength. For parallel excitation we very clearly observe the energy funneling. Each generation shows a distinct bleaching signal as it becomes populated and finally we get a strong bleaching from the trap in combination with little ESA signal. Note however, the differences in the high resolution ($\Gamma = 8\,cm^{-1}$) signal, where different states are predominantly involved in the energy transport. The perpendicular configuration gives a quite different view of the same funneling process. Most notably the trap shows no bleaching at all, since its transition dipole moment is perpendicular to the probe–pulse polarization. In the long time limit we only see the ESA signal and no bleaching.

In conclusion, we have demonstrated that pump–probe experiments provide information about the dynamics of photoexcitations in dendrimeric systems not accessible from time resolved fluorescence. The nonlinear exciton equations and the doorway–window formalism provide a convenient way to simulate these experiments in complex molecules.

Acknowledgements

The support of the Chemical Science Division, Department of energy is gratefully acknowledged.

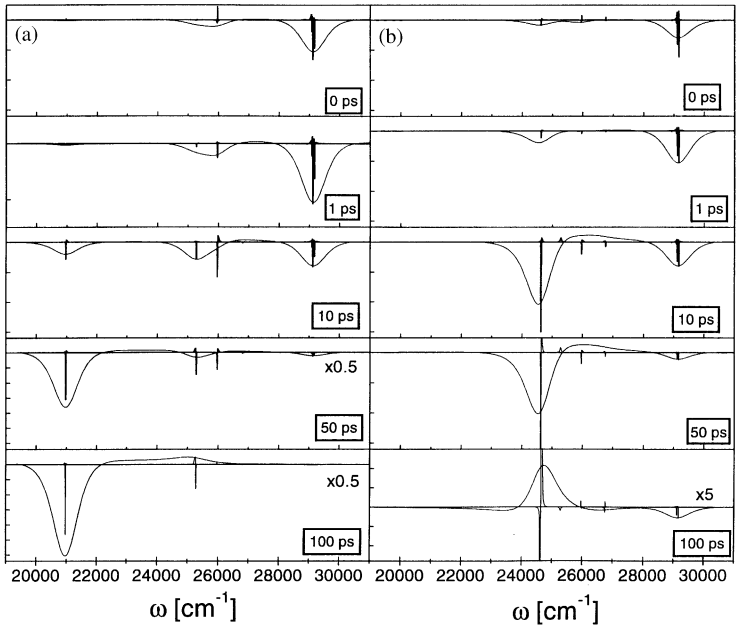

Fig. 4. Polarized pump–probe signals. The pump pulse is always assumed to be parallel to the transition dipole of the trap. The probe is (a) parallel and (b) perpendicular to the pump (note that some of the signals are scaled by the factors indicated).

The stay of A.T. in Rochester was funded by the Austrian Special Research Program F016 "ADLIS" (Austrian Science Foundation Vienna/Austria).

References

[1] A.W. Bosman, H.M. Janssen, E.W. Meijer, Chem. Rev. 99 (1999) 1665.
[2] P.-W. Webber, Y.-J. Liu, C. Devadoss, P. Bharathi, L.S. Moores, Adv. Mater. 8 (1996) 237.
[3] B.M. Junge, D.V. McGrath, Chem. Commun. 9 (1997) 857.
[4] D.A. Tomalia, A.M. Naylor, W.A. Goddard, Angew. Chem. Int. Ed. Engl. 29 (1990) 138.
[5] V.J. Pugh, Q.-S. Hu, L. Pu, Angew. Chem. Int. Ed. 39 (2000) 3638.
[6] R. Kopelman, M. Shortreed, Z.-Y. Shi, W. Tan, Z. Xu, J. Moore, A. Bar-Haim, J. Klafter, Phys. Rev. Lett. 78 (1997) 1239.
[7] M. Shortreed, S.F. Swallen, Z.-Y. Shi, W. Tan, Z. Yu, C. Devadoss, J. Moore, R. Kopelman, J. Phys. Chem. B 101 (1997) 6318.
[8] S. Tretiak, V. Chernyak, S. Mukamel, J. Am. Chem. Soc. 119 (1997) 11,408.
[9] J. Kirkwood, C. Scheurer, V. Chernyak, S. Mukamel, J. Chem. Phys. 114 (2001) 2419.
[10] T. Minami, S. Tretiak, V. Chernyak, S. Mukamel, J. Lumin. 87–89 (1999) 115.
[11] V. Chernyak, W.M. Zhang, S. Mukamel, J. Chem. Phys. 109 (1998) 9587.
[12] A.G. Redfield, Adv. Magn. Reson. 1 (1965) 1.
[13] W.T. Pollard, A.K. Felts, R.A. Friesner, Adv. Chem. Phys. 93 (1997) 77.
[14] V. Chernyak, T. Minami, S. Mukamel, J. Chem. Phys. 112 (2000) 7953.
[15] S. Mukamel, Principles of Nonlinear Optical Spectroscopy, Oxford University Press, New York, 1995.
[16] M. Dahlbom, T. Minami, V. Chernyak, T. Pullerits, V. Sundström, S. Mukamel, J. Chem. Phys. 104 (2000) 3976.
[17] V. Kleiman, J.S. Melinger, S. McMorrow, J. Phys. Chem. B 105 (2001) 5595.
[18] V. Chernyak, E.Y. Poliakov, S. Tretiak, S. Mukamel, J. Chem. Phys. 111 (1999) 4158.
[19] A. Tortschanoff, S. Mukamel, J. Chem. Phys., submitted for publication.